Archival Report

Biological Psychiatry: Celebrating 50 Years

The Selective RhoA Inhibitor Rhosin Promotes Stress Resiliency Through Enhancing D1-Medium Spiny Neuron Plasticity and Reducing Hyperexcitability

T. Chase Francis, Alison Gaynor, Ramesh Chandra, Megan E. Fox, and Mary Kay Lobo

ABSTRACT

BACKGROUND: Nucleus accumbens dopamine 1 receptor medium spiny neurons (D1-MSNs) play a critical role in the development of depression-like behavior in mice. Social defeat stress causes dendritic morphological changes on this MSN subtype through expression and activation of early growth response 3 (EGR3) and the Rho guanosine triphosphatase RhoA. However, it is unknown how RhoA inhibition affects electrophysiological properties underlying stress-induced susceptibility.

METHODS: A novel RhoA-specific inhibitor, Rhosin, was used to inhibit RhoA activity following chronic social defeat stress. Whole-cell electrophysiological recordings of D1-MSNs were performed to assess synaptic and intrinsic consequences of Rhosin treatment on stressed mice. Additionally, recorded cells were filled and analyzed for their morphological properties.

RESULTS: We found that RhoA inhibition prevents both D1-MSN hyperexcitability and reduced excitatory input to D1-MSNs caused by social defeat stress. Nucleus accumbens–specific RhoA inhibition is capable of blocking susceptibility caused by D1-MSN EGR3 expression. Lastly, we found that Rhosin enhances spine density, which correlates with D1-MSN excitability, without affecting overall dendritic branching.

CONCLUSIONS: These findings demonstrate that pharmacological inhibition of RhoA during stress drives an enhancement of total spine number in a subset of nucleus accumbens neurons that prevents stress-related electrophysiological deficits and promotes stress resiliency.

Keywords: Intrinsic excitability, Medium spiny neuron, Nucleus accumbens, RhoA, Social defeat stress, Stress resilience

https://doi.org/10.1016/j.biopsych.2019.02.007

Depression is prevalent globally, and pharmacological treatments for depressed patients vary in their efficacy. Devising new treatments to specifically target functional changes in core brain loci that drive depression, such as the nucleus accumbens (NAc) (1–3), would provide enhanced treatment outcomes. The NAc contains a diverse set of neurons, the majority of which are NAc efferents termed medium spiny neurons (MSNs). These cells are differentiated by their dopamine receptor expression, either D_1 receptor or D_2 receptor expression, and their activity plays differential roles in reward-related behaviors (4–8). D1-MSNs are critical for the expression of anhedonia, a core behavioral symptom in depression (5,9–11). In response to repeated stress, these neurons display electrophysiological adaptations including hyperexcitability, reduced excitatory transmission, and reduced activity (5,10,12). D1-MSN electrophysiological changes appear to be driven by alterations in dendritic morphology (10). Indeed, in rodents (13) and depressed patients (14), the NAc displays significant reductions in volume. It is possible that these volumetric changes could be driven by D1-MSN dendritic atrophy (10,11).

Depression-like behavior caused by chronic stress can be alleviated by blocking both electrophysiological and morphological changes via knockdown of early growth response 3 (EGR3), which regulates neuronal plasticity (4,15–19). EGR3 binds and targets molecules that drive structural complexity in MSNs, including the Rho guanosine triphosphatase RhoA (10). RhoA has been shown to be critically involved in mediating behavioral deficits to social defeat stress (11). However, it is unknown what the effects of RhoA inhibition are on electrophysiological properties underlying depression-like behavior and the relationship between these changes on structural properties in D1-MSNs.

Here, we used a novel, small-molecule Rho–guanosine triphosphatase inhibitor, Rhosin, which selectively targets RhoA (20). By inhibiting RhoA, Rhosin prevents negative cytoskeletal reorganization (21–23) and formation of protrusions such as filopodia without toxic effects (24). We replicated the finding

ISSN: 0006-3223

that systemic and NAc-specific RhoA inhibition blunts behavioral deficits caused by social defeat stress (11). We demonstrate that this stress-resilience relies on restoration of NAc D1-MSN electrophysiological properties underlying depression-like behavior. Additionally, we establish a role for enhanced dendritic spine formation caused by RhoA inhibition in blunting D1-MSN hyperexcitability and preventing depression-like behavior.

METHODS AND MATERIALS

Experimental Subjects

For all electrophysiology and morphological experiments, D1–green fluorescent protein (GFP) or D2-GFP hemizygote mice on a C57BL/6J background were used (25) (GENSAT Project, New York, NY; gensat.org). Drd1a-Cre (D1-Cre) hemizygote mice (line FK150; GENSAT) (26) were used in EGR3 overexpression experiments. For behavioral experiments including sucrose preference, C57BL/6J (Jackson Laboratory, Bar Harbor, ME) mice were used. All experimental mice were male and 8 to 12 weeks of age. Male CD-1 retired breeders (>4 months; Charles River Laboratories, Wilmington, MA), screened for high aggression, were used as aggressors. Studies were conducted in accordance with the Institutional Animal Care and Use Committee at University of Maryland School of Medicine's guidelines.

Social Defeat Stress Procedures and Sucrose Preference

The chronic social defeat stress (CSDS) procedure was performed as previously described (5,10,27). Briefly, each day for 10 days, mice were placed in a cage containing a novel aggressive CD-1 retired breeder for 10 minutes of physical interaction followed by 24 hours of sensory interaction until the next defeat session. The subthreshold social defeat stress procedure was performed as previously described (5,10). Over the course of 1 day, mice were exposed to three novel CD-1 aggressors for 2 minutes per defeat session with 15 minutes of sensory contact after each defeat session. Social interaction behavior was quantified on day 11 (CSDS) or the day after subthreshold social defeat stress and tracked for offline analysis (CleverSys, Reston, VA). Social interaction behavior was performed by placing mice in an open field with an empty perforated box that they were allowed to explore for 2.5 minutes. Immediately after, defeat mice were removed and a novel CD-1 retired breeder was added to the perforated chamber and defeat mice were again placed in the open field (2.5 minutes), and the time that mice spent in an interaction zone around a perforated box was quantified.

Two-bottle choice sucrose preference was administered, as previously (10). Mice were habituated for 2 days to two 50-mL bottles filled with water. On the third day, one water bottle was replaced with a 1% sucrose solution. Bottles were weighed and switched to the opposite side daily. Preference was calculated as percentage of sucrose consumed relative to total liquid consumed over the 2-day sucrose consumption period.

Animal Surgery and Rhosin Administration

For EGR3 overexpression experiments, adeno-associated virus injection was performed as described previously (10) under 0.5% to 1.5% isoflurane anesthesia. For reference to adeno-associated virus construction, see Chandra *et al.* (28). The cre-dependent, double inverted open reading frame virus (adeno-associated virus–double inverted open–EGR3–enhanced yellow fluorescent protein) was injected bilaterally (0.6 μL at a rate of 50 nL/min) in the NAc (anterior-posterior: 1.6 mm, lateral: 1.5 mm, dorsal-ventral: −4.4 mm) of D1-Cre mice. For Rhosin NAc infusion experiments, 4.0-mm bilateral cannulas (Plastics One, Roanoke, VA) were placed above the NAc and affixed with bone screws and dental cement. Notes of cannula placement were taken when mice were sacrificed the day after social interaction. Only mice with cannula tracts above or within the NAc were included in the analysis. Mice recovered in their home cage on heating pads until they were fully ambulatory. All mice were monitored daily and allowed 2 weeks to recover in the animal facility before behavioral testing.

Rhosin was prepared in a 5% dimethylsulfoxide, 0.9% saline solution, gently warmed to dissolve. Vehicle contained a 5% dimethylsulfoxide solution in 0.9% saline. Injections were administered intraperitoneally (IP) at 40 mg/kg 15 minutes prior to physical defeat. For Rhosin administered following defeat, injections were administered one time per day for 7 days, and social interaction was retested on day 8. For cannula infusion, 30 μmol/L Rhosin solution was infused bilaterally at a rate of 0.1 μL/min for a total 0.5 μL infusion on each side.

Immunohistochemistry

Mice expressing EGR3–enhanced yellow fluorescent protein were perfused with 4% paraformaldehyde and incubated in paraformaldehyde overnight and placed in 30% sucrose solution for cryoprotection. Brain slices (35 μm) were sectioned by cryostat (Leica Biosystems, Buffalo Grove, IL). Slices were washed three times for 10 minutes with 1X phosphate-buffered saline (PBS). Slices were blocked in 3% normal donkey serum and 0.3% Triton-X (20%) in 1X PBS. Slices were incubated in rabbit GFP (1:1000; Aves Labs, Davis, CA) primary antibody overnight at room temperature. The next day, slices were washed three times for 15 minutes and incubated in anti-rabbit Alexa 488 (1:1000; Jackson ImmunoResearch Laboratories, West Grove, PA) for 2 hours followed by 1X PBS and mounting with Vectashield 4′,6-diamidino-2-phenylindole (DAPI)–containing mounting media (Vector Laboratories, Burlingame, CA). All slices were imaged on a FV500 confocal microscope (Olympus, Center Valley, PA).

Slice Processing and Dendrite Analysis

Slices and cells were processed and analyzed as previously described (10). Briefly, cells were filled with neurobiotin (0.1%) during whole-cell recording, and slices were immediately fixed in 4% paraformaldehyde following recording. Slices were washed with 1X PBS and blocked in in 10% normal donkey serum and 0.05% Triton X (20%). Slices were incubated overnight in Steptavidin conjugated to Cy3 (#016-160-084; Jackson ImmunoResearch). Slices were washed in 1X PBS and mounted the next day. For dendritic arbor analysis,

Z-stacks were reconstructed with the ImageJ plugin (National Institutes of Health, Bethesda, MD) simple neurite tracer (29). Sholl analysis was performed by counting dendrite intersections with concentric circles. For spines, spines were classified and analyzed using NeuronStudio (Mount Sinai School of Medicine, Computational Neurobiology Imaging Center, New York, NY). Spine counts from secondary dendrites (two or three per cell) were averaged per cell. One or two cells per animal were used for dendrite analysis. For all counts, the experimenter was blinded to behavioral conditions.

Electrophysiology

Isoflurane-anesthetized mice were perfused with, and NAc coronal slices (300 μm) were prepared in, ice-cold oxygenated sucrose artificial cerebrospinal fluid (ACSF) containing (in mmol/L: 194 sucrose, 30 NaCl, 26 $NaHCO_3$, 10 glucose, 4.5 KCl, 3 $MgCl_2$, 1.2 NaH_2PO_4; osmolarity: 330 mOsm). Slices were incubated at 33°C for 1 hour before recording in holding ACSF (in mmol/L: 125 NaCl, 25 $NaHCO_3$, 10 glucose, 3.5 KCl, 3 $MgCl_2$, 1.25 NaH_2PO_4, 0.1 $CaCl_2$; osmolarity: 305–310 mOsm). Sucrose cutting solutions provide a protective cutting method for protection of neurons and provide improved health of striatal neurons relative to sodium-based ACSF solutions (30). For recording, magnesium and calcium in ACSF were 1 mmol/L. Whole-cell recordings were performed under differential interference contrast microscopy visual guidance at 40 times magnification using an Olympus BX61 microscope (Olympus). D1-MSNs or D2-MSNs were identified by visualizing GFP-positive or GFP-negative cells using a mercury arc lamp and a GFP filter. Negative cells were verified to be MSNs by action potential waveforms, low resting membrane potential, and lack of spontaneous firing at baseline. Signals were amplified and digitized using a Mulitclamp 700B amplifier and Digidata 1322 digitizer (20 kHz), respectively (Molecular Devices, Sunnyvale, CA).

Whole-cell recordings utilized a potassium gluconate–based internal solution (in mmol/L: 126 K gluconate, 10 HEPES, 4 KCl, 2 Mg-adenosine triphosphate, 2 Na_2–adenosine triphosphate, 0.3 guanosine triphosphate, 0.2 ethylene glycol tetraacetic acid; osmolarity: 285 mOsm) to fill borosilicate glass pipettes (2–4 MΩ). Rheobase was obtained by injecting a 1-second pulse-ramp. Capacitance was determined by examining charge in capacitive transients in voltage clamp (holding: −70 mV) with a +5 mV, 500-ms voltage deflection (31). Spontaneous excitatory postsynaptic potentials (sEPSPs) were acquired following 5 minutes of cell stabilization prior to excitability recordings. Spontaneous events were deemed to be excitatory by bath application of the α-amino-3-hydroxy-5-methyl-4-isoxazolepropionic acid receptor antagonist CNQX (10 μmol/L) and the *N*-methyl-D-aspartate receptor antagonist APV (50 μmol/L).

RhoA Activation Assay

RhoA activation was determined using a G-LISA (#BK124; Cytoskeleton, Denver, CO) as previously described (11). Briefly, tissue was acquired 2 hours following a 40 mg/kg injection of Rhosin followed by a single defeat. NAc tissue punches using 14-G needles were homogenized with a Pellet Pestle (Thermo Fisher Scientific, Waltham, MA) in lysis buffer, homogenates were centrifuged, and supernatants were snap frozen at −80°C. Protein concentrations were equalized with lysis buffer, and active RhoA determined according to manufacturer's instructions.

Statistical Analysis

Statistics were tabulated using GraphPad Prism 5.0 software (San Diego, CA). For all four group experiments, two-way analyses of variance were used followed by Bonferroni post hoc tests corrected for multiple comparisons. A repeated-measures two-way analysis of variance was used for the spike versus current injection plot. In the legend statistics, *p* values report interaction results unless otherwise specified. Significance on graphs were derived from post hoc tests. For two group statistics, two-tailed *t* tests were used. For cumulative probability plots, Kolmogorov-Smirnov tests were used between groups to calculate differences between distributions. In graphs, individual points represent number of mice in all behavioral experiments, cells in electrophysiological experiments (mice/cells), and cells in morphology experiments. All graphs are represented as mean ± SE measure. Exact statistics can be found in Supplemental Table S1.

RESULTS

Previously, we observed that RhoA is critically involved in mediating behavioral outcomes to social defeat stress (11). To first determine whether the RhoA inhibitor Rhosin would traffic to and be functional in the brain, we injected mice with vehicle or Rhosin (40 mg/kg, IP) 15 minutes prior to a single 10-minute defeat session and collected NAc tissue punches 2 hours following the defeat. Active RhoA was significantly reduced in mice injected with Rhosin compared with vehicle-treated control animals (Supplemental Figure S1A). Next, we characterized general ambulatory and anxiety-like behaviors in response to Rhosin injection by analyzing behavior in an open field. No behavioral differences were observed following Rhosin-injected compared with vehicle-injected mice (Supplemental Figure S1B–E).

A 10-day CSDS procedure was performed on mice destined for electrophysiology or follow-up behavioral measures (Figure 1A). Rhosin (40 mg/kg, IP) or vehicle was systemically administered 15 minutes prior to defeat to block RhoA activation. While defeat significantly reduced the time that experimental mice spent interacting with a novel mouse, Rhosin administration suppressed this effect (Figure 1B) without affecting locomotor behaviors (Figure 1C). A lower dose of Rhosin (20 mg/kg, IP) was not capable of blocking defeat-induced susceptibility (Supplementary Figure S2A). Additionally, Rhosin blocked sucrose preference deficits induced by defeat (Figure 1D). Rhosin alone in the absence of defeat did not affect interaction behavior or sucrose preference (Figure 1B, D). Rhosin (40 mg/kg, IP) administered one time per day for 7 days following social interaction did not reverse deficits that are due to social defeat stress (Supplementary Figure S2B), suggesting that Rhosin blocks the alterations that are due to social defeat, but it likely does not reverse alterations already caused by CSDS.

Next, to determine whether NAc RhoA inhibition could promote resilience to CSDS, the NAc of mice were cannulated

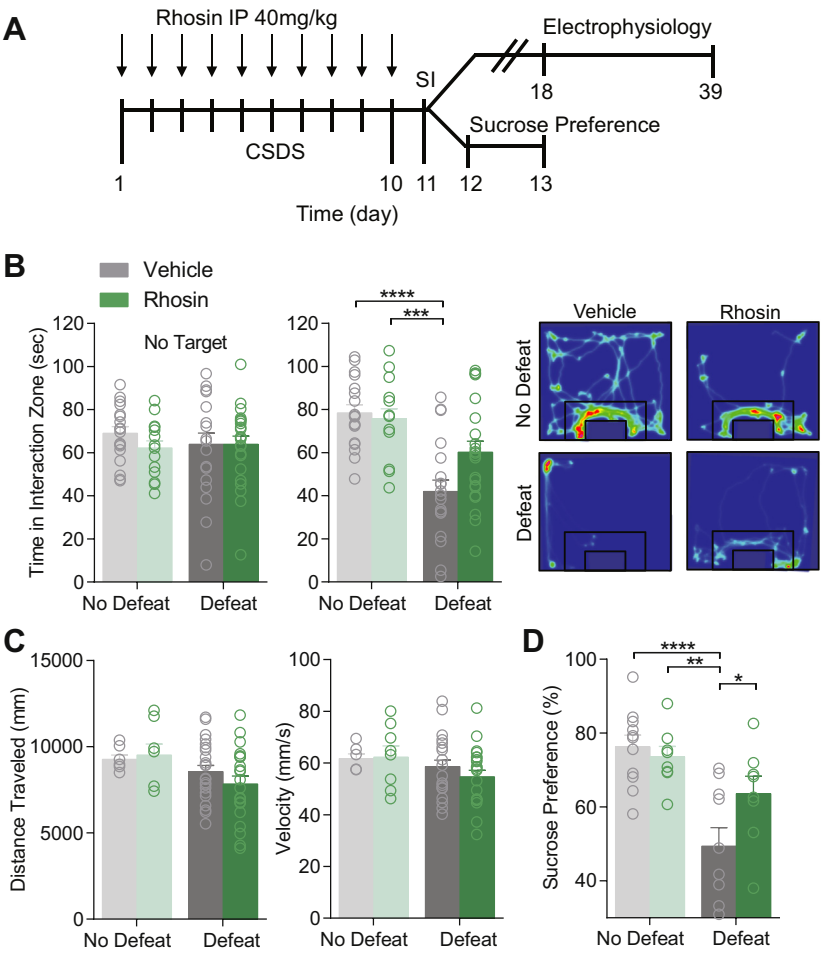

Figure 1. Rhosin blocks stress-induced susceptibility. **(A)** Timeline for chronic social defeat stress (CSDS), social interaction (SI), and subsequent electrophysiology or sucrose preference. **(B)** Rhosin treatment prevents social avoidance caused by social defeat stress (no target: $p > .05$; target: $p < .05$; n = 16–23 mice per group). Representative heat plots display movement of mice around a social target where warm colors represent more time and cool colors represent less time. **(C)** No difference was observed in distance traveled ($p > .05$) or velocity ($p > .05$; n = 16–23 mice per group). **(D)** Rhosin prevented reduced sucrose preference caused by CSDS ($p < .05$; n = 8–11 mice per group). $^{*}p < .05$, $^{**}p < .01$, $^{***}p < .001$, $^{****}p < .0001$. For exact statistics see Supplemental Table S1. IP, intraperitoneal.

and mice were exposed to CSDS (Figure 2A). Fifteen minutes prior to defeat, mice received bilateral, intra-NAc infusions of Rhosin (30 μmol/L) and then were subjected to physical defeat. Rhosin infusion was sufficient to attenuate avoidance behavior (Figure 2B). Previously, we found that overexpression of EGR3 in NAc D1-MSNs was sufficient to promote susceptibility to social defeat stress (10). Two weeks following viral injection and overexpression of EGR3 in D1-MSNs, mice were subjected to subthreshold social defeat stress, a defeat paradigm that normally does not induce depression-like behavior except in vulnerable populations (Figure 2C) (5,10,27). Vehicle or Rhosin (40 mg/kg, IP) was injected 15 minutes prior to the first physical defeat. Rhosin injection was capable of blocking susceptibility caused by EGR3 overexpression in D1-MSNs, suggesting that RhoA inhibition is capable of suppressing NAc EGR3-induced susceptibility.

CSDS causes a persistent (i.e., at least 1-month) enhancement in D1-MSN excitability that corresponds to depression-related behavioral changes (5,10,32). To determine whether systemic Rhosin was capable of preventing this effect, we prepared coronal NAc slices from mice that underwent CSDS and received vehicle or Rhosin injections (Figure 1) and recorded electrophysiological properties from D1-MSNs. Enhanced excitability caused by CSDS was blocked by Rhosin administration as observed by spiking owing to current injection (Figure 3A) and rheobase (Figure 3B). As we found previously, rheobase significantly correlated with time in the interaction zone (Figure 3C) (4). Additionally, the increase in input resistance induced by CSDS was blocked by Rhosin administration (Figure 3D). Smaller-plateau currents by negative current injection were observed in defeat vehicle–treated but not in Rhosin-treated mice (Figure 3E). This result suggests that enhanced input resistance and excitability could be due to a putative potassium channel effect as discussed previously (10). Surprisingly, capacitance still remained reduced in both CSDS vehicle– and Rhosin-treated mice (Figure 3F), indicating that dendritic structural changes may not dictate intrinsic electrophysiological measures. In line with this finding, Rhosin was not capable of restoring dendritic complexity in defeated mice (Figure 4A, B). Additionally, total dendritic length (Figure 4C) and dendritic branch points remained unchanged by Rhosin administration (Figure 4D). No change in soma diameter was found (Figure 4E). These results suggest that changes in rheobase caused by defeat might be mediated by

Biological Psychiatry: Celebrating 50 Years

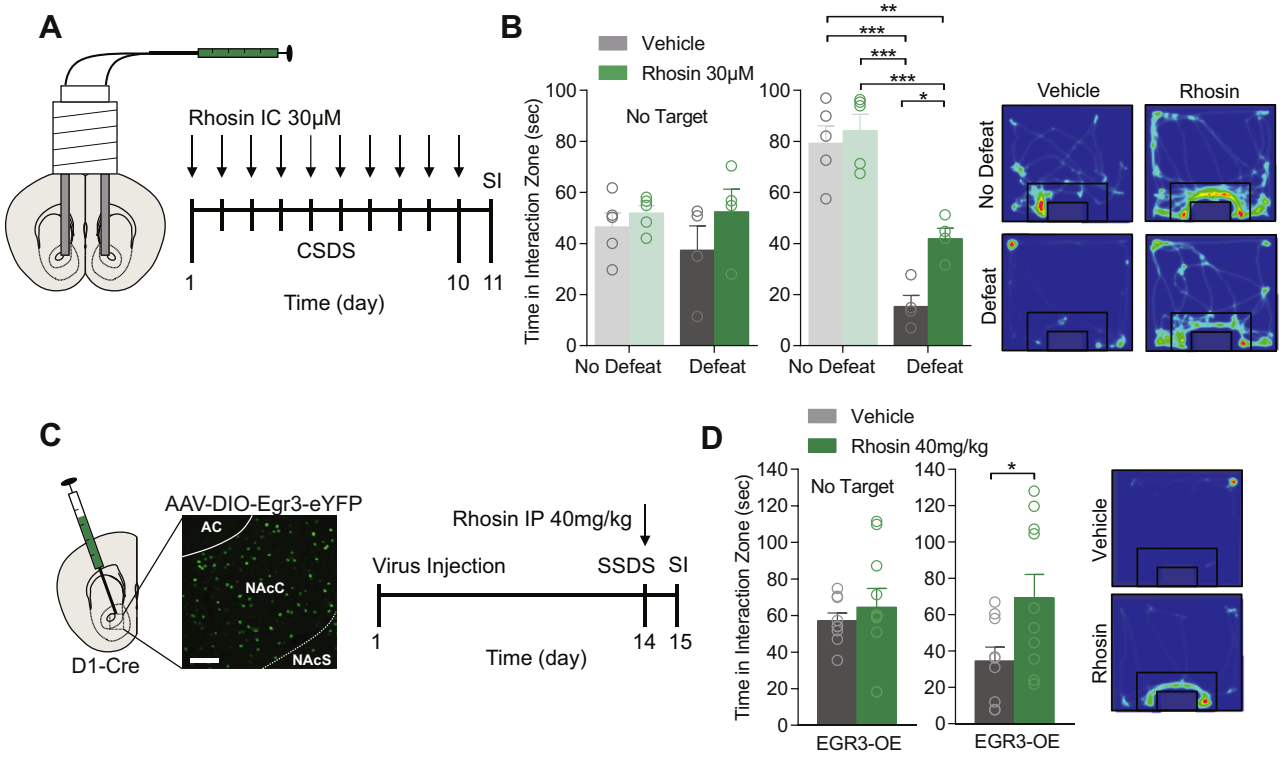

Figure 2. Nucleus accumbens (NAc) Rhosin infusion blocks stress-induced susceptibility and is dependent on dopamine 1 receptor medium spiny neurons early growth response 3 (EGR3) expression. **(A)** Schematic of NAc Rhosin infusion and timeline for treatment. **(B)** Infusion of Rhosin in the NAc attenuates stress-induced social avoidance (no target: $p > .05$; target: $p < .05$; $n = 4–5$ mice per group). **(C)** Injection site of EGR3 overexpression (EGR3-OE) virus within the NAc of Drd1a-Cre (D1-Cre) mice and timeline for treatment (scale bar = 100 μm). **(D)** Subthreshold social defeat stress (SSDS) reduced social interaction (SI) in mice overexpressing EGR3 in NAc dopamine 1 receptor medium spiny neurons, which was blocked by Rhosin treatment ($p < .05$; $n = 9$, 10 mice per group). $^{*}p < .05$, $^{**}p < .01$, $^{***}p < .001$. For exact statistics, see Supplemental Table S1. AAV, adeno-associated virus; AC, anterior commissure; CSDS, chronic social defeat stress; DIO, double inverted open; eYFP, enhanced yellow fluorescent protein; IC, intracranial; IP, intraperitoneal; NAcC, nucleus accumbens core; NAcS, nucleus accumbens shell.

an alternative mechanism that is not dependent on dendritic complexity.

Previously, we found that spontaneous excitatory input was reduced by CSDS in D1-MSNs (5,10). To assess the impact of systemically administered Rhosin on excitatory input, we analyzed sEPSPs prior to acquisition of excitability data. Spontaneous input was deemed to be excitatory, as bath application of the α-amino-3-hydroxy-5-methyl-4-isoxazolepropionic acid receptor blocker CNQX and the *N*-methyl-D-aspartate receptor blocker APV was sufficient to block all spontaneous input (Figure 5A). As observed previously, the frequency of spontaneous excitatory input on NAc D1-MSNs was significantly reduced by CSDS (Figure 5B, C) but did not directly correlate with behavior (Supplemental Figure S3) (4). However, Rhosin administration blocked this effect completely. Defeat significantly enhanced amplitude of sEPSPs but was blocked by Rhosin injection (Figure 5D). Because recordings took place in a potassium-based internal solution, input resistance was increased (Figure 3D), and potassium channel currents were decreased by CSDS (Figure 3E), the enhancement in sEPSP amplitude was likely governed by enhanced input resistance. Additionally, this interpretation is consistent with previous reports of no change in D1-MSN miniature excitatory postsynaptic current amplitude (4,5,10).

Control of excitatory input is, in part, driven by spine density. To determine whether restoration in excitatory transmission and excitability was due to changes in spines, we classified spine types by morphology and quantified the density of spines in all groups. Systemic Rhosin administration significantly enhanced overall spine density in defeated mice as compared with vehicle-treated mice (Figure 6A, B). This enhancement was driven by an increase in thin and mushroom spine density (Figure 6C). Interestingly, rheobase significantly correlated with total spine density (Figure 6D), suggesting that enhanced spine density may play a role in suppressing hyperexcitability caused by CSDS.

DISCUSSION

We have found that selective RhoA inhibition via a novel RhoA inhibitor, Rhosin, can prevent susceptibility to social defeat stress by suppressing stress-induced NAc D1-MSN enhanced excitability and reduced excitatory input. Rhosin prevents electrophysiological changes by enhancing overall spine number, as observed by enhanced spine density. Additionally,

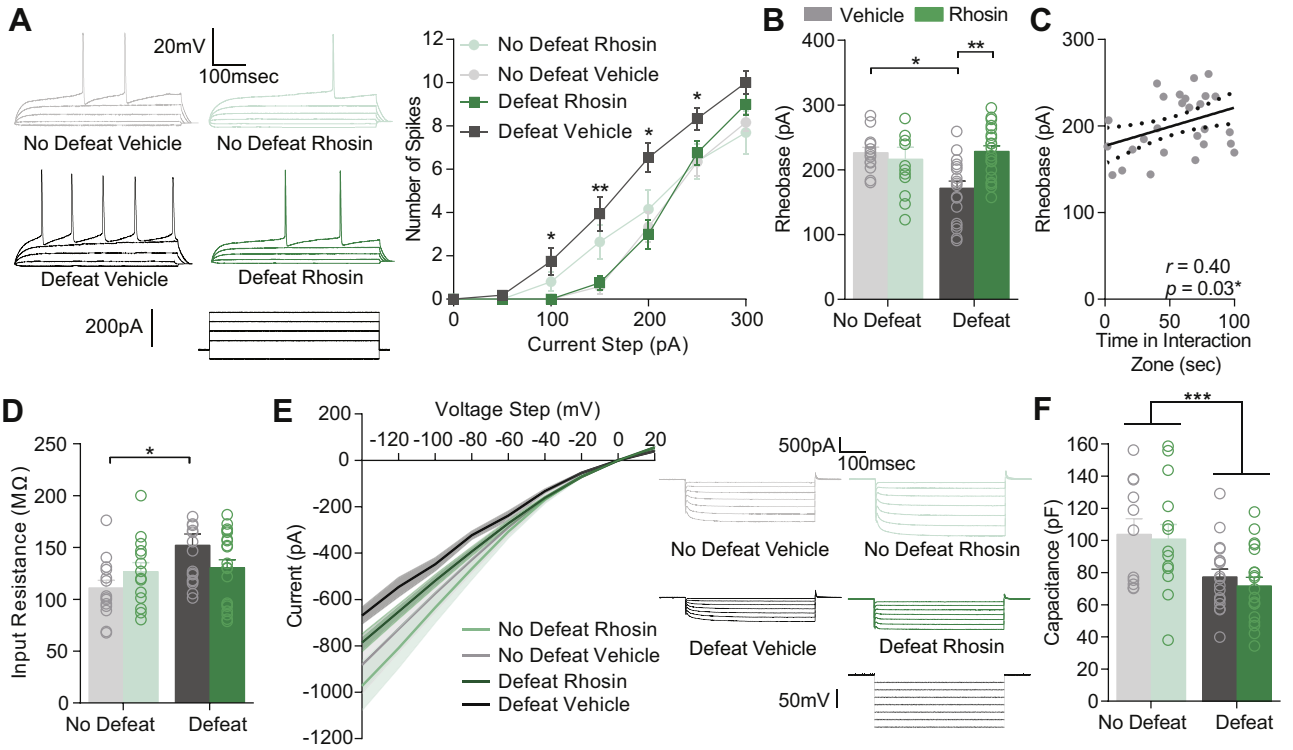

Figure 3. Rhosin blocks stress-induced hyperexcitability in nucleus accumbens dopamine 1 receptor medium spiny neurons. **(A)** Current (−50 to 300 pA) was injected into nucleus accumbens dopamine 1 receptor medium spiny neurons from nondefeat or defeat mice treated with vehicle or Rhosin. Representative traces with current injection (50–200 pA) from each condition are shown. That Rhosin blocked hyperexcitability was observed in defeat mice treated with vehicle ($p < .0001$). **(B)** Reduced rheobase is prevented by Rhosin treatment ($p < .01$). **(C)** Rheobase positively correlates with time spent in the interaction zone ($p < .05$). **(D)** Enhanced input resistance is blocked by Rhosin ($p < .05$). **(E)** Evoked plateau currents (the point at which current stabilizes in response to a negative voltage pulse) from voltage clamp steps (−140 to 20 mV) were smaller in defeat vehicle mice but not in mice treated with Rhosin ($p < .0001$). **(F)** Capacitance was significantly reduced in all defeat animals (interaction: $p > .05$; main effect of defeat: $p < .001$; for all experiments $n = 4–7$ mice/12–20 cells per group). $^*p < .05$, $^{**}p < .01$, $^{***}p < .001$. For exact statistics, see Supplemental Table S1.

this work has demonstrated that NAc EGR3 and RhoA may interact to facilitate susceptibility and that RhoA inhibition can prevent enhanced susceptibility caused by enhanced EGR3 expression. This is consistent with our previous study demonstrating an enrichment of EGR3 binding on the RhoA promoter, suggesting direct transcriptional regulation of RhoA after social defeat stress (10). Additional studies will be necessary to determine whether the direct enhancement of RhoA expression or expression of other facilitatory RhoA signaling molecules drives enhanced RhoA activity through this EGR3 mechanism.

Previous work demonstrated that a RhoA-dependent reduction in NAc dendritic complexity accounts for behavioral effects of social defeat stress (11). While the current findings do not show an overall restoration in dendritic arbor, enhanced spine density is observed. It is likely that the greater total number of spines, whether increased through enhanced spine density or through greater dendritic branching, is sufficient to bring about the social defeat stress effect. For instance, alterations in dendritic arbor on prefrontal cortical neurons caused by stress greatly reduce overall excitatory input, weakening cortical networks (33–35). Driving NAc excitatory afferents or altering excitatory plasticity can reverse physiological and behavioral outcomes to different stress paradigms in a D1-MSN–specific manner (4,36). Therefore, by enhancing overall excitatory activity optogenetically (37) or by transcranial magnetic stimulation (38), both of which produce antidepressant effects, it may be possible to compensate for reduced excitation, thereby normalizing behavior. Analogously, enhancing activity of D1-MSNs optogenetically can promote antidepressant effects (5). Therefore, it is possible that the enhancement in NAc spine density by RhoA may be facilitating similar levels of excitation, and it would be interesting to determine whether RhoA inhibition specifically suppresses D1-MSN synaptic plasticity caused by stress at specific excitatory synapses within the NAc. Additionally, we found that, along with the immature thin spine density enhancement, mushroom spine density was significantly increased. Mushroom spines observed following induction of long-term potentiation (39) are more stable and underlie learning (40,41). In the striatum, increasing the number of stable mushroom spines may provide a means of stabilizing salient, emotional memories (39). Because RhoA plays an antagonistic role in spine formation (42), perhaps a larger proportion of spines are allowed to grow and stabilize over the course of Rhosin injections, providing stronger excitation to

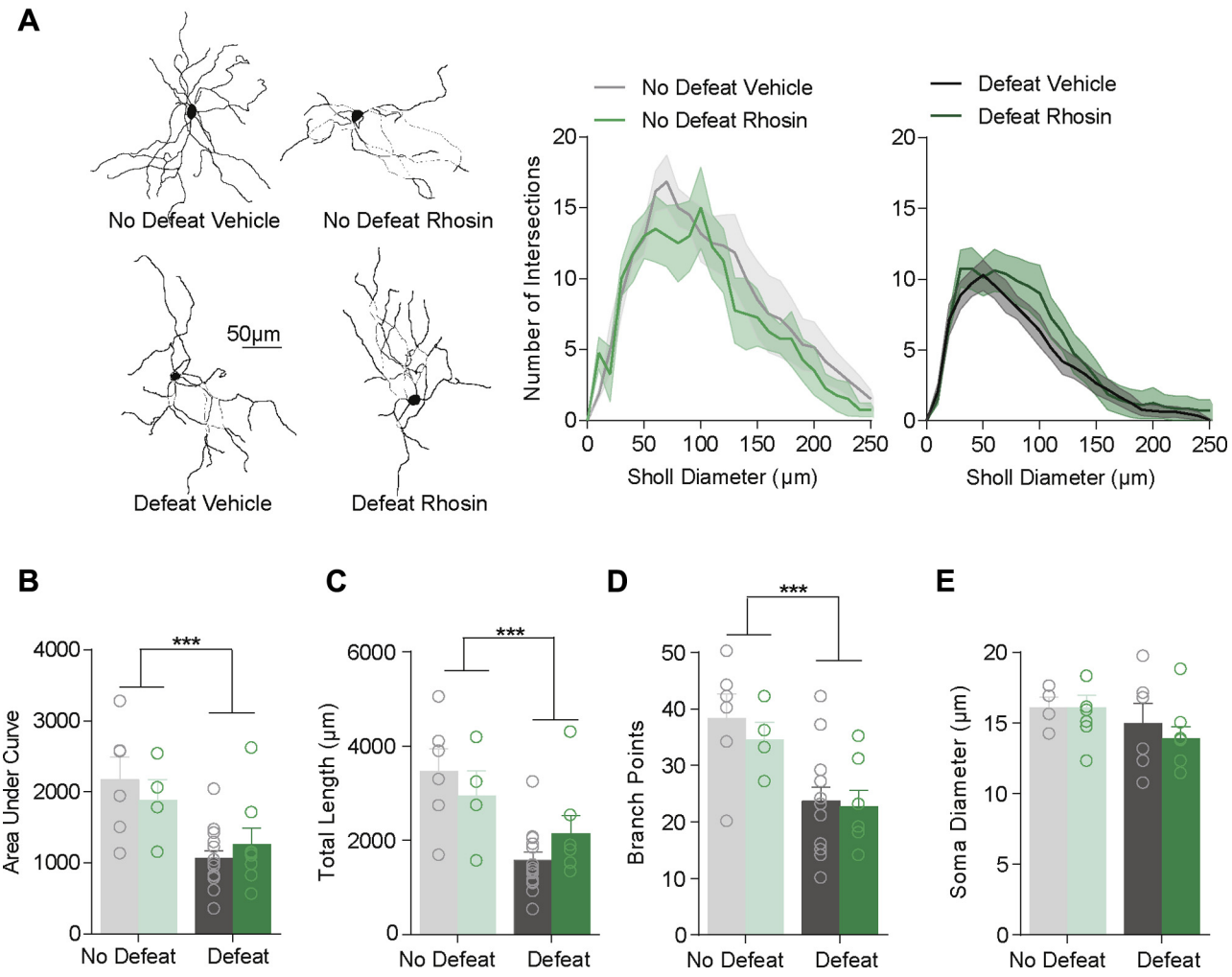

Figure 4. Rhosin has no effect on dendritic atrophy caused by stress. **(A)** Sholl profiles show no treatment difference in concentric ring intersections (10 μm) with dendritic branches. **(B)** No difference in the area under the curve of Sholl plots was observed when comparing across treatment conditions (interaction: $p > .05$; main effect of defeat: $p < .001$). **(C)** Total dendritic length is not different across treatment (interaction: $p > .05$; main effect of defeat: $p < .001$). **(D)** Dendritic branch points are not different across treatment (interaction: $p > .05$; main effect of defeat: $p < .001$; $n = 4–14$ cells per group). **(E)** The soma diameter of cells is not different across defeat or treatment ($p > .05$; $n = 4–9$ cells per group). ***$p < .001$. For exact statistics, see Supplemental Table S1.

D1-MSNs. This has been previously observed in resilient mice that display stronger synaptic strength on mushroom spines in D1-MSNs (43).

MSN subtypes respond and adapt differentially to stress (4,5,9,36). Often, diametric molecular mechanisms drive physiological and behavioral differences in these subtypes (4). For instance, expression of deltaFosB can oppositely alter plasticity in MSN subtypes and enhance spine density in D1-MSN subtypes (44), which may contribute to the reversal of depressive-like behavior (45) or resilience to stress (46) in a similar manner, as we observed. Previous studies have shown a total increase in spine density in mice susceptible to CSDS (12). Our study focuses specifically on spines in D1-MSNs, which may differ from spine density measures on D2-MSNs. We predict that the total enhancement in spine density observed in the NAc may be due to enhanced spine density on D2-MSNs, which is consistent with an increase in miniature excitatory postsynaptic current frequency (5). In D1-MSNs, overall alterations in dendritic structure may play a larger role in mediating physiological and behavioral outcomes to stress.

A critical feature in driving anhedonia is reduced excitatory transmission to NAc D1-MSNs (5,9,10), because D1-MSN activity drives reward (6,7). In vivo D1-MSN activity is diminished following social defeat stress (10), and this attenuation in activity may be driven by an overall reduction in the frequency of excitatory input caused by a loss in the total number of spines. However, reduced excitatory transmission does not directly correlate with stress-induced avoidance (4). Excitatory input and intrinsic excitability coordinate to produce behavior and output from neurons (47). It is possible that a homeostatic mechanism of restoring normal excitatory input in Rhosin-treated mice was sufficient to block hyperexcitability of NAc D1-MSNs. Indeed, rheobase significantly correlates with spine density, suggesting that enhanced

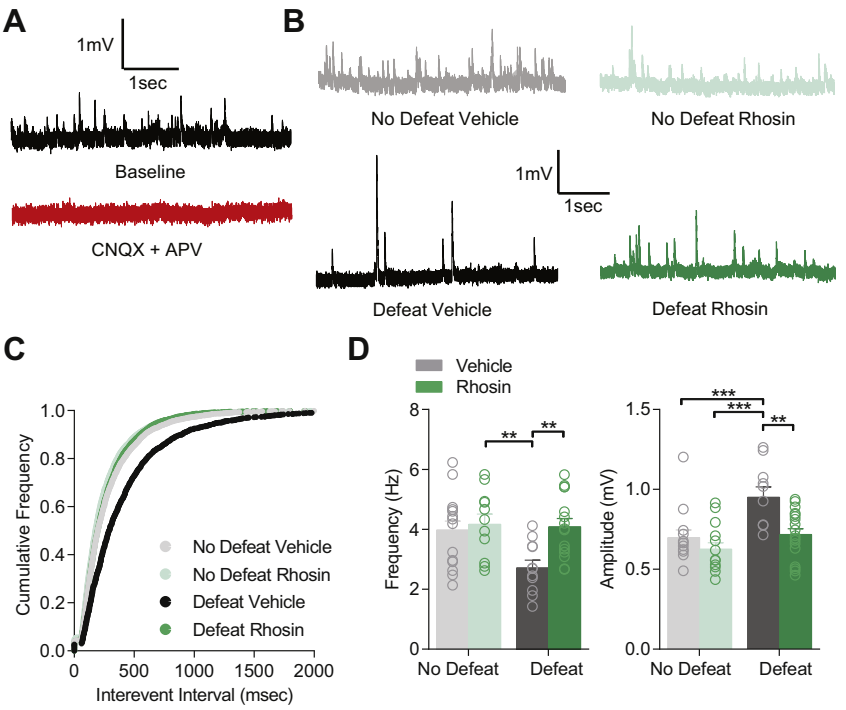

Figure 5. Rhosin prevents decreased excitatory transmission on nucleus accumbens dopamine 1 receptor medium spiny neurons. **(A)** CNQX and APV blocked all spontaneous events, indicating that spontaneous events are excitatory. **(B)** Representative traces of spontaneous excitatory postsynaptic potentials (sEPSPs). **(C)** Cumulative frequency plot demonstrating that Rhosin restored normal sEPSP frequency while vehicle-treated animals displayed elevated frequency (Kolmogorov-Smirnov test defeat Rhosin vs. defeat vehicle: $p < .0001$). **(D)** Rhosin-blocked reduced frequency of sEPSPs ($p < .05$) and enhanced amplitude of sEPSPs ($p < .05$; $n = 3$–6 mice/11–18 cells per group) caused by stress. $^{**}p < .01$, $^{***}p < .001$. For exact statistics, see Supplemental Table S1.

excitatory input onto dendritic spines may prevent hyperexcitability caused by stress. Nevertheless, it is unknown whether changes in excitatory plasticity drive intrinsic changes or vice versa. Future studies will need to examine causal mechanisms linking these two plasticity mechanisms, and their effects on MSN output to connected brain regions. Overall, this study demonstrates an alternative means of restoring electrophysiological properties of D1-MSNs through

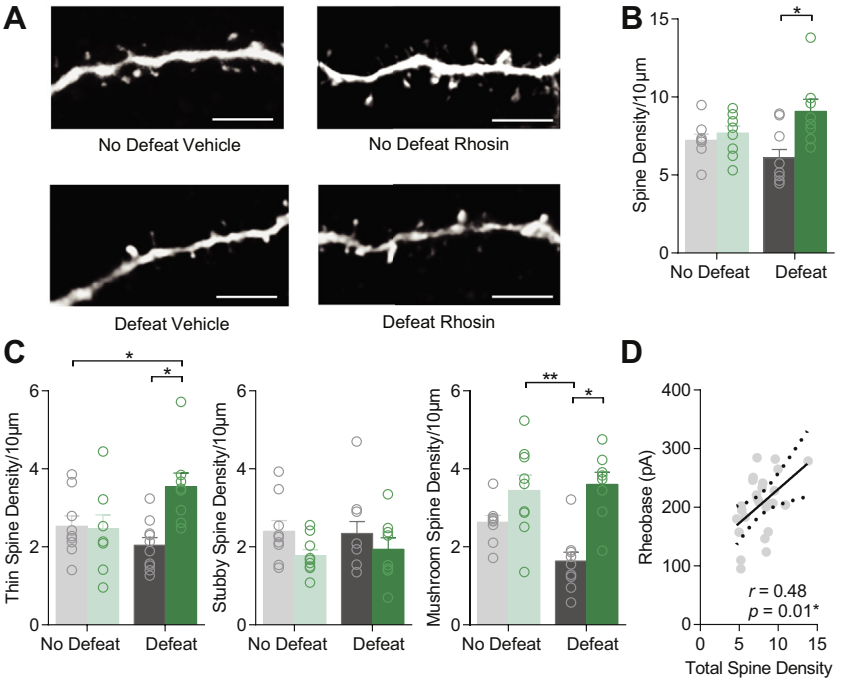

Figure 6. Rhosin enhances spine density in defeat mice. **(A)** Representative images of spines (scale bar = 5 µm). **(B)** Spine density is significantly enhanced by Rhosin treatment in defeat mice ($p < .05$). **(C)** Thin spine density ($p < .05$) and mushroom spine density ($p < .05$), but not stubby spine density ($p > .05$), is enhanced by Rhosin treatment ($n = 8$–10 cells per group). **(D)** Rheobase significantly correlates with total spine density ($p < .05$). $^{*}p < .05$, $^{**}p < .01$. For exact statistics, see Supplemental Table S1.

enhancing overall spine number and excitatory input through inhibition of RhoA.

Rhosin-mediated RhoA inhibition provides a novel means of suppressing behavioral and physiological changes caused by stress without causing deleterious effects in nonstressed mice. While we did not observe a reversal of depression-like behavior in animals treated with Rhosin following stress, Rhosin treatment during stressful events is effective in driving resilience through a physiologically distinct manner. That is, administration prior to stressful events caused an increase in spine density relative to nonstressed conditions, which normalized excitability. Therefore, Rhosin treatment and RhoA inhibition may promote behavioral resilience by allowing for positive actin mobilization and spine formation during stressful events. Rhosin may provide a novel treatment to promote resilience to stress.

ACKNOWLEDGMENTS AND DISCLOSURES

This work was supported by National Institute of Mental Health Grant No. R01MH106500 (to MKL), National Institute on Drug Abuse Grant No. R01DA038613 (to MKL), The One Mind/Janssen Rising Star Translational Research Award (to MKL), National Institute of Mental Health Grant No. F32MH116574 (to MEF), and a National Institute of General Medical Sciences Postdoctoral Research Associate Award 1FI2GM128622-01 (to TCF).

The authors report no biomedical financial interests or potential conflicts of interest.

ARTICLE INFORMATION

From the Department of Anatomy and Neurobiology (TCF, AG, RC, MEF, MKL), University of Maryland School of Medicine; and Synaptic Plasticity Section (TCF), National Institute on Drug Abuse Intramural Research Program, Baltimore, Maryland.

Address correspondence to Mary Kay Lobo, Ph.D., University of Maryland School of Medicine, Department of Anatomy and Neurobiology, 20 Penn Street, HSF2, Room 265, Baltimore, MD 21201; E-mail: mklobo@som.umaryland.edu.

Received Sep 17, 2018; revised Jan 22, 2019; accepted Feb 5, 2019.

Supplementary material cited in this article is available online at https://doi.org/10.1016/j.biopsych.2019.02.007.

REFERENCES

1. Nestler EJ, Barrot M, DiLeone RJ, Eisch AJ, Gold SJ, Monteggia LM (2002): Neurobiology of depression. Neuron 34:13–25.
2. Floresco SB (2015): The nucleus accumbens: An interface between cognition, emotion, and action. Annu Rev Psychol 66:25–52.
3. Russo SJ, Nestler EJ (2013): The brain reward circuitry in mood disorders. Nat Rev 14:609–625.
4. Francis TC, Lobo MK (2017): Emerging role for nucleus accumbens medium spiny neuron subtypes in depression. Biol Psychiatry 81:645–653.
5. Francis TC, Chandra R, Friend DM, Finkel E, Dayrit G, Miranda J, *et al.* (2015): Nucleus accumbens medium spiny neuron subtypes mediate depression-related outcomes to social defeat stress. Biol Psychiatry 77:212–222.
6. Calipari ES, Bagot RC, Purushothaman I, Davidson TJ, Yorgason JT, Pena CJ, *et al.* (2016): In vivo imaging identifies temporal signature of D1 and D2 medium spiny neurons in cocaine reward. Proc Natl Acad Sci U S A 113:2726–2731.
7. Lobo MK, Covington HE 3rd, Chaudhury D, Friedman AK, Sun H, Damez-Werno D, *et al.* (2010): Cell type-specific loss of BDNF signaling mimics optogenetic control of cocaine reward. Science 330:385–390.
8. Lobo MK, Nestler EJ (2011): The striatal balancing act in drug addiction: Distinct roles of direct and indirect pathway medium spiny neurons. Front Neuroanat 5:41.
9. Lim BK, Huang KW, Grueter BA, Rothwell PE, Malenka RC (2012): Anhedonia requires MC4R-mediated synaptic adaptations in nucleus accumbens. Nature 487:183–189.
10. Francis TC, Chandra R, Gaynor A, Konkalmatt P, Metzbower SR, Evans B, *et al.* (2017): Molecular basis of dendritic atrophy and activity in stress susceptibility. Mol Psychiatry 22:1512–1519.
11. Fox ME, Chandra R, Menken MS, Larkin EJ, Nam H, Engeln M, *et al.* (2018): Dendritic remodeling of D1 neurons by RhoA/Rho-kinase mediates depression-like behavior [published online ahead of print Aug 17]. Mol Psychiatry.
12. Christoffel DJ, Golden SA, Dumitriu D, Robison AJ, Janssen WG, Ahn HF, *et al.* (2011): IκB kinase regulates social defeat stress-induced synaptic and behavioral plasticity. J Neurosci 31:314–321.
13. Anacker C, Scholz J, O'Donnell KJ, Allemang-Grand R, Diorio J, Bagot RC, *et al.* (2016): Neuroanatomic differences associated with stress susceptibility and resilience. Biol Psychiatry 79:840–849.
14. Drevets WC, Videen TO, Price JL, Preskorn SH, Carmichael ST, Raichle ME (1992): A functional anatomical study of unipolar depression. J Neurosci 12:3628–3641.
15. Kim JH, Roberts DS, Hu Y, Lau GC, Brooks-Kayal AR, Farb DH, Russek SJ (2012): Brain-derived neurotrophic factor uses CREB and Egr3 to regulate NMDA receptor levels in cortical neurons. J Neurochem 120:210–219.
16. Roberts DS, Hu Y, Lund IV, Brooks-Kayal AR, Russek SJ (2006): Brain-derived neurotrophic factor (BDNF)-induced synthesis of early growth response factor 3 (Egr3) controls the levels of type A GABA receptor alpha 4 subunits in hippocampal neurons. J Biol Chem 281:29431–29435.
17. Li L, Carter J, Gao X, Whitehead J, Tourtellotte WG (2005): The neuroplasticity-associated arc gene is a direct transcriptional target of early growth response (Egr) transcription factors. Mol Cell Biol 25:10286–10300.
18. Li L, Yun SH, Keblesh J, Trommer BL, Xiong H, Radulovic J, Tourtellotte WG (2007): Egr3, a synaptic activity regulated transcription factor that is essential for learning and memory. Mol Cell Neurosci 35:76–88.
19. Gallitano-Mendel A, Izumi Y, Tokuda K, Zorumski CF, Howell MP, Muglia LJ, *et al.* (2007): The immediate early gene early growth response gene 3 mediates adaptation to stress and novelty. Neuroscience 148:633–643.
20. Shang X, Marchioni F, Sipes N, Evelyn CR, Jerabek-Willemsen M, Duhr S, *et al.* (2012): Rational design of small molecule inhibitors targeting RhoA subfamily Rho GTPases. Chem Biol 19:699–710.
21. Zhang XE, Adderley SP, Breslin JW (2016): Activation of RhoA, but not Rac1, mediates early stages of S1P-induced endothelial barrier enhancement. PLoS One 11:1–18.
22. Duan X, Zhang Y, Chen KL, Zhang HL, Wu LL, Liu HL, *et al.* (2018): The small GTPase RhoA regulates the LIMK1/2-cofilin pathway to modulate cytoskeletal dynamics in oocyte meiosis. J Cell Physiol 233:6088–6097.
23. Zaritsky A, Tseng Y-Y, Rabadán MA, Krishna S, Overholtzer M, Danuser G, Hall A (2017): Diverse roles of guanine nucleotide exchange factors in regulating collective cell migration. J Cell Biol 216:1543–1556.
24. Stakaitytė G, Nwogu N, Dobson SJ, Knight LM, Wasson CW, Salguero FJ, *et al.* (2018): Merkel cell polyomavirus small T antigen drives cell motility via Rho-GTPase-induced filopodium formation. J Virol 92:e00940-17. Available at: http://jvi.asm.org/content/92/2/e00940-17.abstract. Accessed September 10, 2018.
25. Gong S, Zheng C, Doughty ML, Losos K, Didkovsky N, Schambra UB, *et al.* (2003): A gene expression atlas of the central nervous system based on bacterial artificial chromosomes. Nature 425:917–925.
26. Gong S, Doughty M, Harbaugh CR, Cummins A, Hatten ME, Heintz N, Gerfen CR (2007): Targeting Cre recombinase to specific neuron populations with bacterial artificial chromosome constructs. J Neurosci 27:9817–9823.

27. Berton O, Mcclung CA, Dileone RJ, Krishnan V, Renthal W, Russo SJ, *et al.* (2006): Essential role of BDNF in the mesolimbic dopamine pathway in social defeat stress. Science 311:864–868.
28. Chandra R, Francis TC, Konkalmatt P, Amgalan A, Gancarz AM, Dietz DM, Lobo MK (2015): Opposing role for Egr3 in nucleus accumbens cell subtypes in cocaine action. J Neurosci 35: 7927–7937.
29. Longair MH, Baker DA, Armstrong JD (2011): Simple neurite tracer: Open source software for reconstruction, visualization and analysis of neuronal processes. Bioinformatics 27:2453–2454.
30. Ting JT, Daigle TL, Chen Q, Feng G (2014): Acute brain slice methods for adult and aging animals: application of targeted patch clamp analysis and optogenetics. Methods Mol Biol 1183:221–242.
31. Golowasch J, Thomas G, Taylor AL, Patel A, Pineda A, Khalil C, Nadim F (2009): Membrane capacitance measurements revisited: Dependence of capacitance value on measurement method in non-isopotential neurons. J Neurophysiol 102:2161–2175.
32. Krishnan V, Han MH, Graham DL, Berton O, Renthal W, Russo SJ, *et al.* (2007): Molecular adaptations underlying susceptibility and resistance to social defeat in brain reward regions. Cell 131:391–404.
33. Radley JJ, Rocher AB, Miller M, Janssen WG, Liston C, Hof PR, *et al.* (2006): Repeated stress induces dendritic spine loss in the rat medial prefrontal cortex. Cereb Cortex 16:313–320.
34. Radley JJ, Anderson RM, Hamilton BA, Alcock JA, Romig-Martin SA (2013): Chronic stress-induced alterations of dendritic spine subtypes predict functional decrements in an hypothalamo–pituitary–adrenal-inhibitory prefrontal circuit. J Neurosci 33:14379–14391.
35. McEwen BS, Morrison JH (2013): Brain on stress: Vulnerability and plasticity of the prefrontal cortex over the life course. Neuron 79:16–29.
36. LeGates TA, Kvarta MD, Tooley JR, Francis TC, Lobo MK, Creed MC, Thompson SM (2018): Reward behaviour is regulated by the strength of hippocampus–nucleus accumbens synapses. Nature 564:258–262.
37. Covington HE, Lobo MK, Maze I, Vialou V, Hyman JM, Zaman S, *et al.* (2010): Antidepressant effect of optogenetic stimulation of the medial prefrontal cortex. J Neurosci 30:16082–16090.
38. McNamara B, Ray JL, Arthurs OJ, Boniface S (2001): Transcranial magnetic stimulation for depression and other psychiatric disorders. Psychol Med 31:1141–1146.
39. Bosch M, Castro J, Saneyoshi T, Matsuno H, Sur M, Hayashi Y (2014): Structural and molecular remodeling of dendritic spine substructures during long-term potentiation. Neuron 82:444–459.
40. Bello-Medina PC, Flores G, Quirarte GL, McGaugh JL, Prado Alcalá RA (2016): Mushroom spine dynamics in medium spiny neurons of dorsal striatum associated with memory of moderate and intense training. Proc Natl Acad Sci U S A 113:E6516–E6525.
41. Bourne J, Harris KM (2007): Do thin spines learn to be mushroom spines that remember? Curr Opin Neurobiol 17:381–386.
42. Tashiro A, Minden A, Yuste R (2000): Regulation of dendritic spine morphology by the rho family of small GTPases: Antagonistic roles of Rac and Rho. Cereb Cortex 10:927–938.
43. Khibnik LA, Beaumont M, Doyle M, Heshmati M, Slesinger PA, Nestler EJ, Russo SJ (2016): Stress and cocaine trigger divergent and cell type-specific regulation of synaptic transmission at single spines in nucleus accumbens. Biol Psychiatry 79:898–905.
44. Grueter BA, Robison AJ, Neve RL, Nestler EJ, Malenka RC (2013): FosB differentially modulates nucleus accumbens direct and indirect pathway function. Proc Natl Acad Sci U S A 110:1923–1928.
45. Vialou V, Robison AJ, Laplant QC, Covington HE 3rd, Dietz DM, Ohnishi YN, *et al.* (2010): DeltaFosB in brain reward circuits mediates resilience to stress and antidepressant responses. Nat Neurosci 13:745–752.
46. Lobo MK, Zaman S, Damez-Werno DM, Koo JW, Bagot RC, DiNieri JA, *et al.* (2013): DeltaFosB induction in striatal medium spiny neuron subtypes in response to chronic pharmacological, emotional, and optogenetic stimuli. J Neurosci 33:18381–18395.
47. Turrigiano GG (2008): The self-tuning neuron: Synaptic scaling of excitatory synapses. Cell 135:422–435.